

GROWTH AND DISSOLUTION OF PORES IN CRYSTALS

R. I. GARBER, V. S. KOGAN, and L. M. POLIAKOV

Physico-Technical Institute, Academy of Sciences, Ukrainian S.S.R.

Submitted to JETP editor June 17, 1958

J. Exptl. Theoret. Phys. (U.S.S.R.) 35, 1364-1368 (December, 1958)

The time dependence of the diffusion processes of sintering and coalescence of pores in rock salt has been determined experimentally. The results agree satisfactorily with the theoretical equations of Lifshitz and Slezov.¹ Numerical values have been determined for the parameters characterizing diffusion in rock salt. It is shown that sintering results not only from the dissolution of pores and direct emergence of vacancies on the free surface, but also via an intermediate stage wherein vacancies accumulate on macrodefects with subsequent formation of large "negative crystals" of the latter. Coalescence of pores has been observed in annealed single crystals of metallic samples, the method of preparation of which (distillation in vacuum, iodide method etc.) caused the initial fine porosity.

IN crystals with high concentrations of vacancies the number of vacancies is reduced by processes which occur during annealing, such as (1) sintering by the escape of excess vacancies to the outside surfaces of sample s, and (2) coalescence of excess vacancies to form macroscopic pores.

Lifshitz and Slezov¹ have studied the kinetics of grain growth in substances precipitated from supersaturated solid solutions, a special case of this being the kinetics of pore growth in a crystal containing excess vacancies. It was shown that during the annealing of such crystals the following two competing processes take place:

1. Far from the crystal boundary, pore growth obeys the law

$$\bar{R}^3 = 4/9 D_v \alpha \tau. \quad (1)$$

2. Near the boundary, pores dissolve in a zone whose width ξ depends on time according to the equation

$$\xi(\tau) = 2 (D_v \alpha \tau)^{1/3} / Q_0^{1/2}. \quad (2)$$

These are asymptotic equations, being applicable only to sufficiently long times, when the pores have become relatively large, when there is small supersaturation, and coalescence occurs (large pores "devouring" small pores). The following notation has been used: D_v is the coefficient of vacancy diffusion, τ is the annealing time, Q_0 is the total initial supersaturation (vacancies plus voids),

$$\alpha = \sigma V c_0 / kT, \quad (3)$$

σ is the surface tension, V is the volume of a single vacancy and c_0 is the (equilibrium) vacancy concentration.

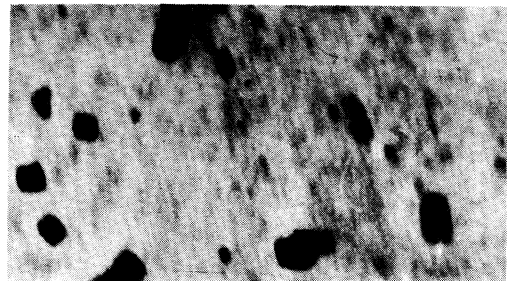


FIG. 1. Cleavage plane of initial rock salt sample. Magnification 25000 \times .

It should be noted that, unlike the usual equations of the type $\xi(\tau) \sim \tau^{1/2}$ that describe diffusion processes, in the present case the time dependence of the characteristic linear size is given by $\xi(\tau) \sim \tau^{1/3}$.

Pore formation in the body of a crystal during annealing and the growth of a pore-free zone near the surface were previously observed in rock salt.² It was of interest to determine the quantitative laws of these processes experimentally, for comparison with the theoretical equations (1) and (2).

As in reference 2, our samples were transparent rock salt crystals without apparent internal defects but with a fine mosaic pattern and $\sim 0.1 \mu$ pores which could be observed with an electron microscope but not optically. These pores were a source of vacancies for the growth of the larger pores which clouded the sample. Large pores were formed on the boundaries of mosaic blocks. In the electron-microscope photograph (Fig. 1) of a cleavage plane of an initial sample in microscopic pores are squares or rectangles with rounded corners.

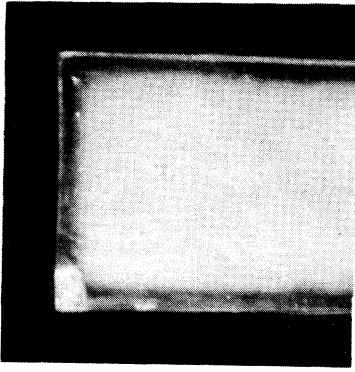


Fig. 2. Transmission photograph of rock salt crystal after annealing at 500°C for 43 hr. Magnification 8×.

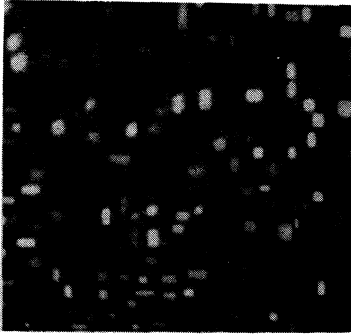


FIG. 3. Pores created on the surface of a mosaic block in the middle of a sample after annealing at 500°C for 43 hr. Magnification 600×.

Our samples permitted microscopic observation and measurement of pore sizes in the interior and of the thickness of the sintered zone on the surface. The pore-free sintered region is clearly revealed by transmitted light because of its transparency, in contrast with the interior of the crystal, which scatters light because of the formation of pores whose dimensions are greater than the wavelengths of visible light (Fig. 2).

The samples were 8×10×25 mm parallelepipeds, annealed in a muffle furnace at 420, 500, 650 and 750°C. The crystals were placed in a thick-walled ceramic tube where equilibrium vapor pressure of the salt was maintained during the anneal. At definite time intervals samples were removed from the furnace together with the tube, thus insuring slow cooling, and microscope measurements were made of the thickness ξ of the transparent surface region in different cross sections. The samples were also split along a cleavage plane, and a metallographic microscope with ocular micrometer was used to measure pore dimensions within the crystals (Fig. 3). Eight to ten values of the sintered zone thickness ξ_i in different cross sections and several pore sizes R_i were averaged to give the plots of $\xi(\tau)$ and $\bar{R}^3(\tau)$ in Figs. 4 and 5.

The curves of $\xi(\tau)$ for individual cross sections of a sample are parallel to the curve of average values within the limits indicated in Fig. 4. Whenever macrodefects in the form of cracks appeared close to the surface the character of the time dependence of transparent zone growth changed

FIG. 4. Thickness of sintered zone as a function of time. Annealing temperature: 1) 500°C; 2) 650°C.

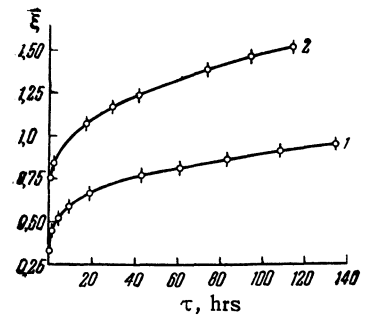
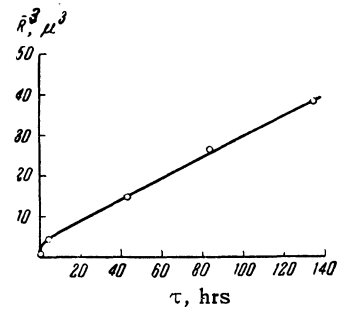


FIG. 5. Pore size as a function of annealing time. Annealing temperature $t = 500^\circ\text{C}$.



since vacancies accumulated at the defects. The average value $\bar{\xi}$ was determined without including values for the transparent zone in cross sections passing through these defects.

Assuming that the width $\bar{\xi}$ of the transparent zone is a power function of time, the exponent n of τ was determined from the experimental curves and compared with the theoretical formula (2). The latter is valid only for sufficiently large τ ; it was therefore impossible to use absolute values of the experimental coordinates on the curves. The power exponent was determined from the relation

$$\Delta\bar{\xi}/\Delta\tau = nA\tau^{n-1}. \quad (4)$$

Figure 6 shows straight lines representing the function $\ln(\Delta\bar{\xi}/\Delta\tau) = f(\ln \tau)$ plotted from the curves of Fig. 4 for 420, 500, 650, and 750°C (Curves 1, 2, 3, and 4). The slope of these curves gives $n = 0.31 \pm 0.02$,* which is in good agreement with the theoretical value 0.33.

The curve of $\bar{R}^3(\tau)$ in Fig. 5 also agrees with the theoretical relation (1). By means of Eq. (1), derived for spherical pores, the slope of the straight portion of this curve can be utilized to determine $D_V\alpha = D_Vc_0 \sigma V/kT$ and thus to estimate the atomic diffusion coefficient

$$D = D_Vc_0.$$

The mean volume of vacancies in the rock salt lat-

*The range of values of n is determined from the spread of experimental points, taking into account the error in measuring the width of the transparent zone ($\delta\bar{\xi}(\tau) = \pm 0.02$ mm).

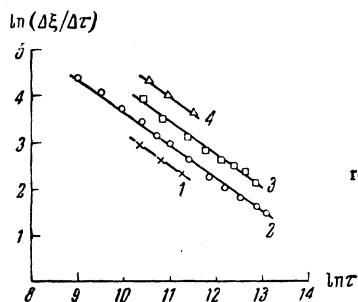


FIG. 6. Graphs of the relation $\ln(\Delta\xi/\Delta\tau) = f(\ln \tau)$.

tice is $V = 1.15 \times 10^{-23} \text{ cm}^3$. For mosaic crystals of rock salt we can assume $\sigma = 10^3 \text{ erg/cm}^2$.³ With these values of V and σ , $D = 3.1 \times 10^{-9} \text{ cm}^2/\text{sec}$ for 500°C.

Since the experimental relation for $\bar{\xi}(\tau)$ agreed with the theoretical relation (2), we have $A = 2(D\alpha)^{1/3}/Q_0^{1/2}$ in Eq. (4). By using the value of A obtained from the line intersecting the $\ln(\Delta\xi/\Delta\tau)$ axis in Fig. 6 (Curve 2) and the value of D for the same temperature (500°C), we obtain the total initial supersaturation $Q_0 = 2.2 \times 10^{-4}$. This is the relative volume of voids in the crystal after annealing. Figure 3 provides an independent means of determining the volume of pores per unit of mosaic block surface. The volume of pores on the surface of a block (of linear size $\sim 10^{-2} \text{ cm}$) divided by its total volume agrees with the calculated value of Q_0 .

Pore size in the zone next to the transparent region at the free surface is the critical value at which pore dissolution begins. From the knowledge of this value we can use the expression for critical pore size,⁴

$$R^* = c_0 2\sigma V / \Delta c kT, \quad (5)$$

to determine the degree of supersaturation in the crystal.

Assuming $R^* = 3 \times 10^{-4} \text{ cm}$ and $V = 1.15 \times 10^{-23} \text{ cm}^3$, we obtain

$$\Delta c / c_0 = 0.7 \cdot 10^{-3},$$

which agrees with the values given in other papers.⁴

By combining data on the relation between transparent zone thickness and annealing time at 420, 650, and 750°C (Curves 1, 3, and 4 of Fig. 6) with the value of D at 500°C (Curve 2 of Fig. 6) we ob-

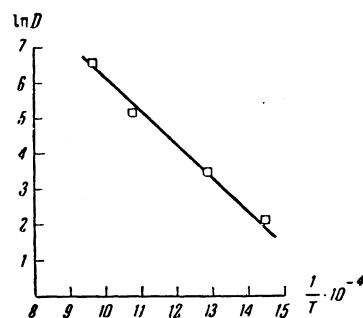


FIG. 7. Graph of $\ln D = f(1/T)$.

tained the diffusion coefficients at all of these temperatures (see the table).

The data in the table and the graph of $\ln D = f(1/T)$ plotted therefrom (Fig. 7) were used to determine the activation energy of diffusion in rock salt, $E = 19,000 \text{ cal/g-atom}$ and the exponential coefficient $D_0 = 6.8 \times 10^{-4} \text{ cm}^2/\text{sec}$. Since in the given rock salt crystals the pores were located on the boundaries of mosaic blocks and the diffusion processes which cause coalescence and sintering also occur on the boundaries of these blocks, the diffusion coefficients and activation energies obtained above apply to boundary diffusion.

Annealing at high temperatures (750°C and above) induces a rapid growth of pores inside the crystal, which produces local transparency and the growth of the transparent zone on the surface. Local transparency in the interior occurs principally around separate defects, where pores are formed through the accumulation of vacancies.

Under prolonged annealing the transparent regions merge, and the entire crystal becomes transparent. In that event some pores may remain within the crystal and continue to grow because of defects. Such pore growth has been observed in an annealed rock salt crystal containing a macrocrack. Figure 8 is a transmission photograph of pores formed on a crack after 18-hour annealing at 760°C. These pores are spherical cavities into which the crack was divided through surface tension.

Annealing for 75 hours induces some increase of pore size; the pores acquire crystallographic

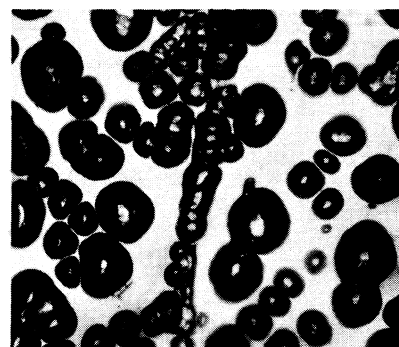


FIG. 8. Crack in rock salt after annealing at 760°C for 18 hr.

Temperature, °K	Diffusion coefficient, cm^2/sec
693	$7.9 \cdot 10^{-10}$
773	$3.1 \cdot 10^{-9}$
923	$1.6 \cdot 10^{-8}$
1023	$0.7 \cdot 10^{-7}$



FIG. 9 The same crack as in Fig. 8, but after annealing at 760°C for 75 hr. Magnification 37×.



FIG. 10. "Negative crystal" in rock salt after annealing at 760-790°C for 200 hr. Magnification 21×.



FIG. 11. Iron single crystal after annealing in vacuum at 1000°C for 42 hr. Magnification 315×.

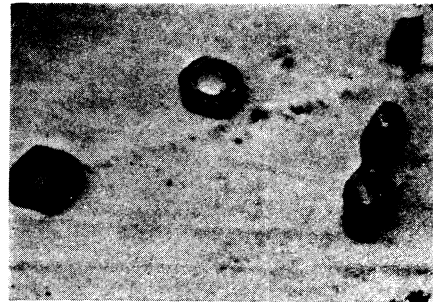


FIG. 12. Magnesium single crystal after annealing at 400 to 420°C for 60 hr. Magnification 420×.

faces and neighboring pores coalesce (Fig. 9). At this stage internal defects serve as sites for vacancy accumulation, competing with the free surface. These defects grow into large "negative crystals". Figure 10 shows such a "crystal" (~2 mm) with clearly perceptible faces in the (100) and (110) planes which resulted from annealing for 200 hours at 760 to 780°C.

Coalescence of pores is also observed in metal crystals with high vacancy concentration or high initial porosity. Such crystals are produced, for example, from the gases of some metals in vacuum distillation or from the decomposition of their iodides.

Figures 11 and 12 show pores formed in single crystals of iron and magnesium that were produced by vacuum distillation and subsequently annealed. The iron was annealed in vacuum for 42 hours at 1000°C; the magnesium was annealed for 60 hours at 400 to 420°C. The original samples had small pores (3 to 5 μ) without clearly defined crystallographic faces. The annealed samples were ground down 1 to 1.5 mm and the surfaces were used for the sections shown in the photographs.

The section of the iron crystal in Fig. 11 reveals well-defined rectangular pores arranged in lines that coincide with the directions of single-crystal growth during precipitation. Single-crystal iron needles apparently grow in the form of blocks parallel to the needle axis. Large pores form on the surfaces of these blocks. Magnesium sections

(Fig. 12) clearly show large pores with six faces (20 to 25 μ) on block surfaces. The pore faces possess a stepped fine structure that is clearly visible in the photograph. Zirconium produced by the iodide method also contains six-sided pores. Rectangular pores on block surfaces have also been observed in a nickel single crystal produced by vacuum distillation.

Pores appear during the annealing of crystals which, depending on the method of production, possess excess vacancies or initial fine porosity. Pores have not been observed in compact metal castings subjected to annealing.

The authors wish to thank Professor I. M. Lifshitz and V. V. Slezov for discussions of the results, and V. K. Sklyarov for experimental assistance.

¹I. M. Lifshitz and V. V. Slezov, *J. Exptl. Theoret. Phys. (U.S.S.R.)* 35, 479 (1958), *Soviet Phys. JETP* 8, 331 (1959).

²Garber, Kogan, and Poliakov, *Физика металлов и металловедение (Physics of Metals and Metal Research)* 4, 89 (1957).

³V. D. Kuznetsov, *Поверхностная энергия твердых тел (Surface Energy of Solids)*, GITTL, 1954.

⁴Ya. E. Geguzin, *Usp. Fiz. Nauk.* 61, 217 (1957).